AGU PUBLICATIONS

Geochemistry, Geophysics, Geosystems

RESEARCH ARTICLE
10.1002/2016GC006628

The biokarst system and its carbon sinks in response to pH changes: A simulation experiment with microalgae

Tengxiang Xie[1,2] and Yanyou Wu[1]

[1]State Key Laboratory of Environmental Geochemistry, Institute of Geochemistry, Chinese Academy of Sciences, Guiyang, Guizhou, China, [2]State Key Laboratory of Marine Environmental Science, Xiamen University, Xiamen, Fujian, China

Key Points:
- The three key processes of biokarst system were completely quantitatively described in a wide range of pH conditions from 6 to 9
- Successfully estimated the rate of biodissolution and DIC utilization amount from calcite dissolution by microalgae in different pH
- Found out the variation in biokarst carbon sink, photosynthetic carbon sink, and total carbon sink with pH change

Supporting Information:
- Table S1
- Table S2
- Figure S1

Correspondence to:
Y. Wu,
wuyanyou@mail.gyig.ac.cn

Citation:
Xie, T. and Y. Wu (2017), The biokarst system and its carbon sinks in response to pH changes: A simulation experiment with microalgae, *Geochem. Geophys. Geosyst.*, *18*, 827–843, doi:10.1002/2016GC006628.

Received 6 SEP 2016
Accepted 30 NOV 2016
Accepted article online 20 DEC 2016
Published online 3 MAR 2017

Abstract This study aims to explore the changes in a microalgal biokarst system as a potential carbon sink system in response to pH changes. The bidirectional isotope labeling method and mass balance calculation were adopted in a simulated biokarst environment with a series of set pH conditions and three microalgal species. Three key processes of the microalgal biokarst system, including calcite dissolution, $CaCO_3$ reprecipitation, and inorganic carbon assimilation by microalgae, were completely quantitatively described. The combined effects of chemical dissolution and species-specific biodissolution caused a decrease in overall dissolution rate when the pH increased from 7 to 9. $CaCO_3$ reprecipitation and the utilization of dissolved inorganic carbon originating from calcite dissolution decreased when the pH increased from 7 to 9. The three processes exhibited different effects in changing the CO_2 atmosphere. The amount of photosynthetic carbon sink was larger at high pH values than at low pH values. However, the CO_2 sequestration related to the biokarst process (biokarst carbon sink) increased with decreasing pH. Overall, the total amount of sequestered CO_2 produced by the biokarst system ($CaCO_3$-CO_2-microalgae) shows a minimum at a specific pH then increases with decreasing pH. Therefore, various processes and carbon sinks in the biokarst system are sensitive to pH changes, and biokarst processes play an important negative feedback role in the release of CO_2 by acidification. The results also suggest that the carbon sink associated with carbonate weathering cannot be neglected when considering the global carbon cycle on the scale of thousands of years (<3 ka).

1. Introduction

Biokarst, including carbonate dissolution, $CaCO_3$ precipitation, and inorganic carbon assimilation, is a complex and important process in karst areas [*Taylor et al*., 1979; *Yuan*, 2001]. There is a viewpoint that the chemical weathering of silicate rocks is a major process in terms of feedback interactions with atmospheric CO_2 drawdown over periods of thousands to millions of years, whereas the weathering of carbonate rocks is thought to be unimportant because all CO_2 consumed in the dissolution of carbonates is returned to the atmosphere by the reprecipitation of carbonates in the oceans ($Ca^{2+}+2HCO_3^- \leftrightarrow CaCO_3+CO_2+H_2O$) [*Berner et al*., 1983; *Elderfield*, 2010]. However, some recent studies have shown that when aquatic organisms take part in the karst process, the role of karst in CO_2 consumption cannot be ignored due to the much faster kinetics of dissolution and the uptake of weathering-related dissolved inorganic C (DIC) by aquatic photosynthesis on the thousands year timescale [*Kump et al*., 2000; *Liu et al*., 2011]. Based on field monitoring results and theoretical calculations, the combined effects of carbonate dissolution, the water cycle, and photosynthetic utilization of dissolved inorganic carbon (DIC) by aquatic organisms have contributed up to 0.8242 Pg C·a^{-1} of the global atmospheric CO_2 [*Gombert*, 2002; *Liu et al*., 2010; *Meybeck*, 1993], especially in karst rivers containing carbonates and aquatic organisms. Microalgae, as the main primary producers of biokarst in lakes and oceans, is actively involved in adjusting carbonate dissolution and $CaCO_3$ precipitation rates and the uptake of weathering-related DIC [*Lerman and Mackenzie*, 2005; *Wang et al*., 2014; *Xie and Wu*, 2014].

Due to the effects of acidic wastewater discharge and acid rain, the seasonal pH range of natural karst lakes has shifted from between pH 8 and 9 to between pH 6 and 9 [*Chetelat et al*., 2008; *Han et al*., 2010]. This decrease in pH can change the carbonate system equilibrium of the lakes, leading to CO_2 release ($HCO_3^- + H^+ \leftrightarrow CO_2 + H_2O$). Meanwhile, the pH variations strongly influence not only carbonate dissolution and $CaCO_3$ precipitation but also the physiological activity of microalgae. The three-step reaction rate

constants (k_1, k_2, k_3, and k_{-3}) corresponding to simple carbonate chemical dissolution are strongly dependent on pH [*Chou et al*., 1989; *Plummer and Wigley*, 1976]. Moreover, inorganic carbon uptake, enzyme activity, and microalgal photosynthesis are also affected by pH [*Azov*, 1982; *Li et al*., 2012; *Menéndez et al*., 2001] and further influence biokarst processes. Therefore, studies on how pH affects biokarst processes with respect to microalgae is essential for us to understand the role of biokarst systems in terms of the CO_2 consumed under different pH conditions.

Most studies have focused on one or two of these processes, while few have simultaneously described all three. Moreover, most previous studies have assessed total effects instead of distinguishing between chemical and biological effects when investigating biokarst systems, and few studies have directly observed microalgae utilize carbon from carbonates or have determined the utilization amount. Therefore, obtaining a thorough understanding of the biological functions of a biokarst system at different pH values is difficult.

The bidirectional isotope labeling method and mass balance modeling were adopted in a simulated karst environment to examine a wide range of pH conditions. The dissolution of carbonate minerals, reprecipitation of $CaCO_3$, and assimilation of inorganic carbon were quantitatively described at different pH values to gain insight into the response of the biokarst system to different pH conditions and its role in CO_2 adjusted.

2. Materials and Methods

2.1. Materials

Two types of low-magnesium calcites (referred to as calcite) were collected: one from Anshun, Guizhou, China (calcite-1) and the other from Wulong, Chongqing, China (calcite-2). All samples were fresh and free from weathering. They possessed similar chemical compositions but different stable carbon isotope compositions ($\delta^{13}C$), because of one is marine origin (Calcite-1) and the other is of freshwater origin (Calcite-2) (Table 1). The chemical compositions were determined via XRF (analytical precision was better than 3%). The measurement of $\delta^{13}C$ was performed using MAT-252 (Finnigan, Bremen, Germany) via "the method of phosphoric acid" (analytical precision was better than 0.2 ‰) [*McCrea*, 1950]. The calcite samples were cleaned, air-dried, and crushed in a shatter box equipped with a tungsten carbide grinding container. The crushed calcite samples were sieved to isolate fractions with sizes between 0.2 and 0.3 mm. To remove fine-grained particles from the crushing process, we ultrasonically washed the sieved samples repeatedly in ultrapure water (at least five times) and then dried them at 50°C to obtain a constant weight for experimental use. All $\delta^{13}C$ data were reported relative to PDB.

Three typical species of microalgae in karst lakes were chosen, namely *Chlamydomonas reinhardtii* (*C.R.*), *Chlorella pyrenoidosa* (*C.P.*), and *Microcystis aeruginosa* (*M.A.*) [*Wu et al*., 2008]. They were obtained from the Institute of Hydrobiology, Chinese Academy of Sciences and cultured in a greenhouse at the Institute of Geochemistry, Chinese Academy of Sciences. They were grown axenically in an artificial freshwater soil extract (SE) medium containing 0.25 $g{\cdot}L^{-1}$ $NaNO_3$, 0.075 $g{\cdot}L^{-1}$ $K_2HPO_4{\cdot}3H_2O$, 0.075 $g{\cdot}L^{-1}$ $MgSO_4{\cdot}7H_2O$, 0.025 $g{\cdot}L^{-1}$ $CaCl_2{\cdot}2H_2O$, 0.175 $g{\cdot}L^{-1}$ KH_2PO_4, 0.025 $g{\cdot}L^{-1}$ NaCl, 0.0005 $g{\cdot}L^{-1}$ $FeCl_3{\cdot}6H_2O$, 1 $mL{\cdot}L^{-1}$ EDTA-Fe (0.82 $mL{\cdot}L^{-1}$ HCl, 0.1802 $g{\cdot}L^{-1}$ EDTA-Na_2, and 0.9010 $g{\cdot}L^{-1}$ $FeCl_3{\cdot}6H_2O$), 1 $mL{\cdot}L^{-1}$ trace metal solution (2.86 $g{\cdot}L^{-1}$ H_3BO_3, 1.86 $g{\cdot}L^{-1}$ $MnCl_2{\cdot}4H_2O$, 0.22 $g{\cdot}L^{-1}$ $ZnSO_4{\cdot}7H_2O$, 0.39 $g{\cdot}L^{-1}$ $Na_2MoO_4{\cdot}2H_2O$, 0.08 $g{\cdot}L^{-1}$ $CuSO_4{\cdot}5H_2O$, and 0.05 $g{\cdot}L^{-1}$ $Co(NO_3)_2{\cdot}6H_2O$], and 40 $mL{\cdot}L^{-1}$ soil extract solution (200 $g{\cdot}L^{-1}$ soil). All the samples were incubated at 25.0°C ± 1.0°C under a light intensity of 150 $\mu mol{\cdot}m^{-2}{\cdot}s^{-1}$ with a 12/12 h day/night cycle.

2.2. Experimental Procedure

After incubation, the microalgae was transferred to the modified SE medium, which was depleted in soil extract and Ca^{2+} and contained only 30% Mg^{2+}, for 2 days before each experiment to facilitate their

Table 1. The Chemical Compositions and $\delta^{13}C$ Values of Calcites

Sample	Fe_2O_3 (wt. %)	MgO (wt. %)	CaO (wt. %)	K_2O (wt. %)	MnO (wt. %)	P_2O_5 (wt. %)	L.O.I (wt. %)[a]	TOTAL (wt. %)	$\delta^{13}C$ (‰)
Calcite-1	0.04	0.94	54.81		0.07		44.66	100.52	0.72
Calcite-2		0.32	55.26	0.003		0.09	44.71	100.38	−10.29

[a]L.O.I: loss on ignition.

Table 2. Experiment Treatments

Microalgae	Calcite (0.5 g)	pH Treatments[e]
Control[a]	Calcite-1[c] or Calcite-2[d]	6[f] 7[f] 8[f] 9[f]
C.R. or *C.P.* or *M.A.*[b]	Calcite-1[c] or Calcite-2[d]	6[f] 7[f] 8[f] 9[f]

[a]*Control*: The treatment without microalgae.
[b]*C.R*, *C.P*, and *M.A*: The treatments with *C. reinhardtii* (*C.R.*), *C. pyrenoidosa* (*C.P.*), and *M. aeruginosa* (*M.A.*).
[c]Calcite-1: The treatments added 0.5g Calcite-1.
[d]Calcite-2: The treatments added 0.5g Calcite-2.
[e]Adjusted pH by adding small amounts of 0.1 mol·L^{-1} HCl every 6 h.
[f]6, 7, 8, and 9: The treatments with a controlled pH (6, 7, 8, and 9).

adaptation to the experimental conditions and to prevent the release of excess Ca^{2+} and Mg^{2+} caused by imbalance between the internal and external cellular environments at the beginning of the experiment.

The experiments were conducted in 250 mL Erlenmeyer flasks with aseptically sealed membranes. Approximately 10 mL of the microalgae solution ($OD_{680} = 3$, the optical density of algal at 680 nm), 0.5 g of calcite, and 140 mL of the modified SE medium at different pH values were added. Details of the experimental treatments are listed in Table 2. All treatments were conducted using three replicates.

At 6, 24, 48, 72, 120, and 168 h of culture, 10 mL aliquots were obtained to determine Mg^{2+}, Ca^{2+}, and chlorophyll-a concentrations. After harvest (168 h), 20, 10, and 60 mL aliquots were used to determine algal Mg^{2+} and Ca^{2+} concentrations, the quantity of nonpurgeable organic carbon (NPOC) and stable carbon isotopic compositions ($\delta^{13}C$), respectively. The detailed analysis procedures of the parameters are described in section 2.3.

A pH meter (Youke PHS-3C, Shanghai, China), equipped with a glass electrode with a precision of ±0.01 pH units, was used to monitor pH changes in the culture medium. The pH of the culture medium was adjusted by adding small amounts of 0.1 mol·L^{-1} HCl every 6 h. Less than 5 mL of HCl was added throughout the entire experimental process, and approximately 3.6 mmol·L^{-1} Cl^- was added to the culture medium during harvest time. *Chen et al*. [2009] reported that the photosynthetic rates of *Synechocystis* and *M. aeruginosa* are unaffected by 100 mmol·L^{-1} Cl^- under conditions with 10 mmol·L^{-1} DIC, and the rates decreased by only approximately 17% at 100 μmol·L^{-1} DIC in the presence of 20 mmol·L^{-1} Cl^-. Thus, the effect of Cl^- on microalgae could be ignored.

2.3. Sample Analysis

2.3.1. Determination of Mg^{2+}, Ca^{2+}, and Chlorophyll-a Concentrations After Different Durations of Incubation

The 10 mL samples were centrifuged, decanted, and filtered (0.22 μm, polyethersulfone). The filtrate was analyzed for Ca^{2+} and Mg^{2+} concentrations using ICP–OES (Vista MPX, USA) (analytical precision was better than ±5%). The chlorophyll a (chl-a) concentration in the algae precipitate was measured using a UV spectrophotometer (Labtech UV-2000, Boston, USA) [*Huang and Cong*, 2007].

2.3.2. Determination of Algal Mg^{2+} and Ca^{2+} Concentrations Following Different Treatments

After harvest (168 h), 20 mL aliquots were obtained from the culture medium. The samples were centrifuged, and the supernatant was decanted. Approximately 20 mL of 95% ethyl alcohol was added to the centrifuge tube containing the algae precipitate to extract chlorophyll [*Huang and Cong*, 2007]. After 24 h in the dark, the extracted solution was centrifuged, and the supernatant was collected to measure the algal chl-a concentration. Approximately 10 mL of 0.1 mol·L^{-1} HCl was added to the centrifuge tube containing the algae precipitate to dissolve the remnant calcite particles. After the calcite was completely dissolved, it was centrifuged, the supernatant was decanted, and the precipitate was mixed with the chlorophyll extraction solution. Finally, the mixture was poured into a 40 mL Teflon cup, and the ethyl alcohol was evaporated off by placing the cup on an electric hot plate set at 80°C. After the ethyl alcohol was completely volatilized, the precipitate was digested via high-pressure hydrothermal decomposition (HNO_3:H_2O_2 = 2:1), and its Ca^{2+} and Mg^{2+} concentrations were measured using ICP–OES (Vista MPX, USA) [*Huang and Schulte*, 1985; *Topper and Kotuby-Amacher*, 1990]. The algal Mg^{2+} and Ca^{2+} concentrations were determined using the following equations:

$$C_{PCa} = \frac{C_{Ca}}{C_{ch-a}} \text{ or } C_{pMg} = \frac{C_{Mg}}{C_{chl-a}} \quad (1)$$

where Cp_{Ca} and Cp_{Mg} are the Ca^{2+} and Mg^{2+} contents of one chl-a unit of algae (mg·μg^{-1}), respectively; C_{Ca} and C_{Mg} are the Ca^{2+} and Mg^{2+} contents of algae per unit culture medium (mg·L^{-1}), respectively; and $C_{chl\text{-}a}$ is the chl-a content of algae per unit culture medium (μg·L^{-1}).

2.3.3. Measurements of Algal Stable Carbon Isotopic Composition ($\delta^{13}C$) and Nonpurgeable Organic Carbon (NPOC)

After harvest (168 h), the NPOC in 10 mL algal culture aliquots was measured via thermal catalysis using an Elementar High TOC II-analyzer (Hanau, Germany). The remaining algal cultures were centrifuged, the supernatant was decanted, and the precipitate was treated with 1 mol·L^{-1} of HCl to eliminate inorganic carbon then dried via vacuum freeze-drying prior to analysis. Quartz tubes were loaded with the samples and CuO, and were evacuated, sealed, and heated at 850°C for 5 h [*Buchanan and Corcoran*, 1959]. Water and oxygen were removed from the gas stream using a mixture of an alcohol and liquid N_2 trap and a liquid N_2 trap, and CO_2 was double-distilled and collected into a sample tube via a glass high-vacuum line [*Boutton*, 1991]. $\delta^{13}C$ measurements were performed on the extracted CO_2 using a MAT-252 (Finnigan, Bremen, Germany). The analytical precision was ±0.2‰. All data were reported as per mill (‰) relative to PDB, as shown in equation (2).

$$\delta^{13}C(\%) = \left(\frac{R_{\text{sample}}}{R_{\text{standard}}} - 1\right) \cdot 1000 \tag{2}$$

where R_{sample} and R_{standard} are the ratios of the heavy to light isotopes ($^{13}C/^{12}C$) of the sample and the standard, respectively.

2.4. Calculation Methods

2.4.1. Total Amount of Ca^{2+} or Mg^{2+} Within the Culture Medium and Algae Body

The total amounts of Ca^{2+} or Mg^{2+} within the culture medium and algae body per unit volume medium at *i* sampling time were determined using the following equation:

$$T_i = C_i + Ch_i \cdot C_p \quad (i = 6,\ 24,\ 48,\ 72,\ 120\ \textit{and}\ 168\ \text{h}) \tag{3}$$

where T_i (mg·L^{-1}) is the total amount of Ca^{2+} or Mg^{2+} within the culture medium and algae body per unit volume medium at *i* sampling time; C_i (mg·L^{-1}) is the Ca^{2+} or Mg^{2+} concentration of the culture medium at *i* sampling time; Ch_i (μg·L^{-1}) is the concentration of algal chl-a in the culture medium at *i* sampling time; and *Cp* (mg·μg^{-1}) is the Ca^{2+} or Mg^{2+} content of one chl-a unit of algae corresponding to the treatment.

2.4.2. Amount of Released Mg^{2+} Per Unit of Algae Based on Chl-a Content Per Unit Time

To eliminate physical and chemical dissolution effects when calculating the biological dissolution, we initially calibrated the Mg^{2+} concentrations in the solution with the Mg^{2+} concentration of the initial culture medium and control groups:

$$CT_i = C_i \cdot \frac{C_0}{CO_i} \quad (i = 6,\ 24,\ 48,\ 72,\ 120\ \text{and}\ 168\ \text{h}) \tag{4}$$

where CT_i and C_i (mg·L^{-1}) are the concentrations of Mg^{2+} in the culture medium treated with both calcite and algae before and after the calibration at the same sampling time, respectively; CO_i (mg·L^{-1}) is the concentration of Mg^{2+} in the culture medium containing only calcite at the same sampling time (control); C_0 (mg·L^{-1}) is the initial concentration of Mg^{2+} in the culture medium; and *i* is the sampling time [*Xie and Wu*, 2014].

Then, the amount of Mg^{2+} released by the algae at *i* sampling time per unit volume medium was determined. The value can be obtained from the following equation:

$$N_i = (CT_i - C_0) + (Ch_i - Ch_0) \cdot C_p \tag{5}$$

Afterward, an equation corresponding to the concentration of algal chl-a (Ch_i) in the culture medium over time (*T*) was established (SigmaPlot 10.0) as $Ch_i = Ch(T)$. An equation accounting for biological cumulative action time (PT_i) with respect to culture time was then obtained by integrating the equation of algal chl-a ($Ch(T)$) with time (*T* in hours):

$$PT_i = \int_0^T Ch(T)\ d(T) \tag{6}$$

Finally, the PT_i at different culture times was calculated using equation (6). An equation relating N_i to PT_i was established (SigmaPlot 10.0) as $N_i = N(PT_i)$, and the amount of Mg^{2+} released per unit algae based on chl-a content per unit time (P_i) was obtained from the derivatives of N_i and PT_i, as follows:

$$P_i = \frac{d(N(PT_i))}{d(PT_i)} \tag{7}$$

2.4.3. Calculation of Newborn cell $\delta^{13}C$ During the Treatment

The algae harvested at the end of the treatment included both inoculated algae and newborn algae produced during the treatment. Newborn algal $\delta^{13}C$ values reflect the effect of treatment more accurately than measured algal $\delta^{13}C$ values. Thus, to more accurately represent the varied experimental data, we used an isotope mixing model to determine the newborn algal $\delta^{13}C$ values. The measured algal $\delta^{13}C$ values for each treatment were calibrated as follows:

$$\left(\frac{N_0}{N}\right) \cdot \delta^{13}C_{N0} + \left(1 - \frac{N_0}{N}\right) \cdot \delta^{13}C_{NA} = \delta^{13}C_N \tag{8}$$

where N_0 and N are the NPOC contents at inoculation and after harvest, respectively; $\delta^{13}C_{N0}$ and $\delta^{13}C_N$ are the measured algal $\delta^{13}C$ values at inoculation and after harvest, respectively; and $\delta^{13}C_{NA}$ is the calibrated algal $\delta^{13}C$ value for each treatment, i.e., the newborn algal $\delta^{13}C$ value. The algal $\delta^{13}C$ values used in the subsequent parts of this study are the calibrated algal $\delta^{13}C$ values under each treatment condition.

2.4.4. Proportion of Microalgal Inorganic Carbon Utilization From Calcite Dissolution

Stable carbon isotope analysis is widely used as a biomarker in matter source and food web research [*Boschker and Middelburg*, 2002; *Radajewski et al*., 2000]. Under the above experimental conditions, algae can utilize DIC from two sources, namely, from calcite dissolution and from the atmosphere. Based on a two end-member isotope mixing model, an equation representing this utilization of two different carbon sources by microalgae can be established as follows:

$$\delta^{13}C_{NA} = (1 - f_B) \cdot \delta^{13}C_A + f_B \cdot \delta^{13}C_B \tag{9}$$

where $\delta^{13}C_{NA}$ is the calibrated algae $\delta^{13}C$ value; f_B is the proportion of DIC utilization from calcite dissolution; $\delta^{13}C_A$ is the $\delta^{13}C$ value corresponding to algae entirely using DIC from atmospheric CO_2; and $\delta^{13}C_B$ is the $\delta^{13}C$ value corresponding to algae entirely using DIC from calcite dissolution.

$\delta^{13}C_A$ and $\delta^{13}C_B$ are difficult to determine because of isotopic fractionation. Thus, two types of carbon isotope-labeled calcites (i.e., calcite-1 and calcite-2) were added to two flasks under the same treatment conditions. The equations corresponding to each treatment can be established as follows:

$$\delta^{13}C_{NA1} = (1 - f_{B1}) \cdot \delta^{13}C_{A1} + f_{B1} \cdot \delta^{13}C_{B1} \tag{10}$$

$$\delta^{13}C_{NA2} = (1 - f_{B2}) \cdot \delta^{13}C_{A2} + f_{B2} \cdot \delta^{13}C_{B2} \tag{11}$$

where $\delta^{13}C_{NA1}$ and $\delta^{13}C_{NA2}$ are the algal $\delta^{13}C$ values under cultivation with the first and second labeled calcites under the same treatment conditions, respectively; f_{B1} and f_{B2} are the proportions of DIC utilization from the dissolution of the first and second labeled calcites, respectively; $\delta^{13}C_{A1}$ and $\delta^{13}C_{B1}$ are the algal $\delta^{13}C$ values from the algae entirely using DIC from atmospheric CO_2 and from the dissolution of the first labeled calcite, respectively; and $\delta^{13}C_{A2}$ and $\delta^{13}C_{B2}$ are the algal $\delta^{13}C$ values from the algae entirely using DIC from atmospheric CO_2 and from the dissolution of the second labeled calcite, respectively.

The concentration and $\delta^{13}C$ value of atmospheric CO_2 are identical in the two Erlenmeyer flasks containing the different labeled calcites under the same treatment conditions. Therefore, $\delta^{13}C_{A1} = \delta^{13}C_{A2} = \delta^{13}C_A$. Moreover, the proportions of DIC utilization from calcite dissolution are the same under the same treatment and environmental conditions regardless of the carbon isotope-labeled calcite added. Therefore, $f_{B1} = f_{B2} = f_B$. Based on these two facts, equations (10) and (11) can be rewritten as equation (12)

$$f_B = \left(\delta^{13}C_{NA1} - \delta^{13}C_{NA2}\right) / \left(\delta^{13}C_{B1} - \delta^{13}C_{B2}\right) \tag{12}$$

where $\delta^{13}C_{B1}$ and $\delta^{13}C_{B2}$ are the algal $\delta^{13}C$ values from algae entirely using DIC from the dissolution of the first and second labeled calcites as their unique carbon sources, respectively. The processes of calcite dissolution and DIC utilization by microalgae will produce carbon isotope fractionation effects. The value of carbon isotope fractionation ($\triangle$) is difficult to obtain accurately. However, the carbon isotope fractionation value of the total process, from calcite dissolution to DIC utilization by microalgae, is virtually identical in the two flasks under the same treatment and environmental conditions but with different carbon isotope-

labeled calcites, i.e., $\delta^{13}C_{B1} - \delta^{13}C_{C1} = \triangle_{B1\text{-}C1}$, $\delta^{13}C_{B2} - \delta^{13}C_{C2} = \triangle_{B2\text{-}C2}$, and $\triangle_{B1\text{-}C1} = \triangle_{B2\text{-}C2}$ ($\delta^{13}C_{C1}$: the $\delta^{13}C$ value of the first labeled calcite; $\delta^{13}C_{C2}$: the $\delta^{13}C$ value of the second labeled calcite).

Therefore, $(\delta^{13}C_{B1} - \delta^{13}C_{B2})$ in equation (12) can be replaced with $(\delta^{13}C_{C1} - \delta^{13}C_{C2})$, and equation (12) can be rewritten as follows:

$$f_B = \left(\delta^{13}C_{NA1} - \delta^{13}C_{NA2}\right) / \left(\delta^{13}C_{C1} - \delta^{13}C_{C2}\right) \quad (13)$$

3. Results

3.1. Variations in Chl-a Concentrations at Different pH Values

Various observations of the correlation between chl-a concentration and algal biomass have led to the acceptance of utilizing chl-a analysis as an indirect measure of phytoplankton biomass [*Vörös and Padisák*, 1991]. Chl-a concentrations gradually increased over time for each treatment during the entire cultivation period (Figure 1). However, pH variations differentially affected the growth of different types of microalgae (Figure 1). At pH 7–9, there were no clear differences in the chl-a concentrations in *C.R.*, but they were higher than those at pH 6 (Figure 1). In the *C.P.* incubations, the pH in the culture medium did not have a marked effect on the chl-a concentration (Figure 1). For *M.A.*, the chl-a concentration was the highest at pH 7 and the lowest at pH 9 (Figure 1). In treatments at pH 6 and 8, the chl-a concentrations of *M.A.* exhibited no clear differences (Figure 1).

3.2. Variations in Ca^{2+} and Mg^{2+} Quantities Within Culture Media and Algae Bodies at Different pH Values

When Ca^{2+} or Mg^{2+} was released from the calcite, it was either contained in the culture medium or absorbed by the algae. Therefore, the Ca^{2+} or Mg^{2+} quantities in the culture media and algae bodies directly reflect calcite dissolution.

As shown in Figure 2, the Ca^{2+} quantities in the culture media and algae bodies increased over time and with decreasing pH. However, the rates of increase varied between different treatments. At pH 6, the rate of increase was significantly faster than at other pH values. In addition, there were faster rates of Ca^{2+} increase in the treatments with microalgae than in those without microalgae, especially at pH 7–9 (Figure 2). Under alkaline conditions, $CaCO_3$ solubility is reduced, and chemical dissolution is weaker. Therefore, the effects of microalgae are more apparent at pH 7–9. When comparing algal species, *M.A.* and *C.P.* led to higher increases in Ca^{2+} quantities than did *C.R.* (Figure 2).

Mg^{2+} quantities within the culture media and algae bodies also generally increased over time (Figure 3). Mg^{2+} quantities decreased with increasing pH in the treatments using *C.R.* and in those without microalgae

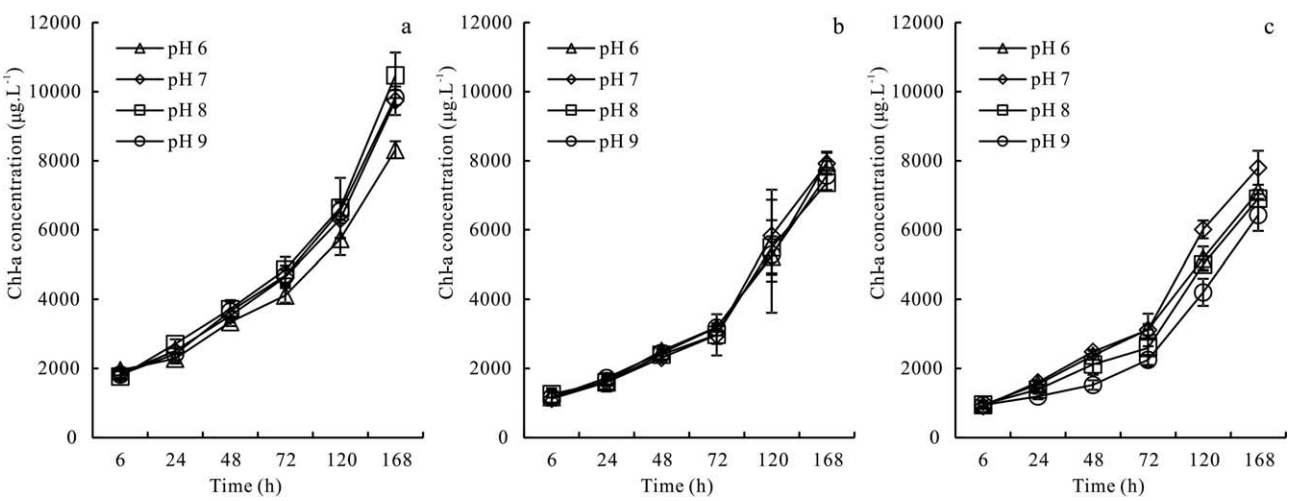

Figure 1. Variations in chl-a concentrations at different pH values after different times (h) of incubation ($\mu g \cdot L^{-1}$). (a) The treatment with *C. reinhardtii* (*C.R.*), (b) the treatment with *C. pyrenoidosa* (*C.P.*), and (c) the treatment with *M. aeruginosa* (*M.A.*). Error bars in Figures 1a–1c) correspond to 1σ.

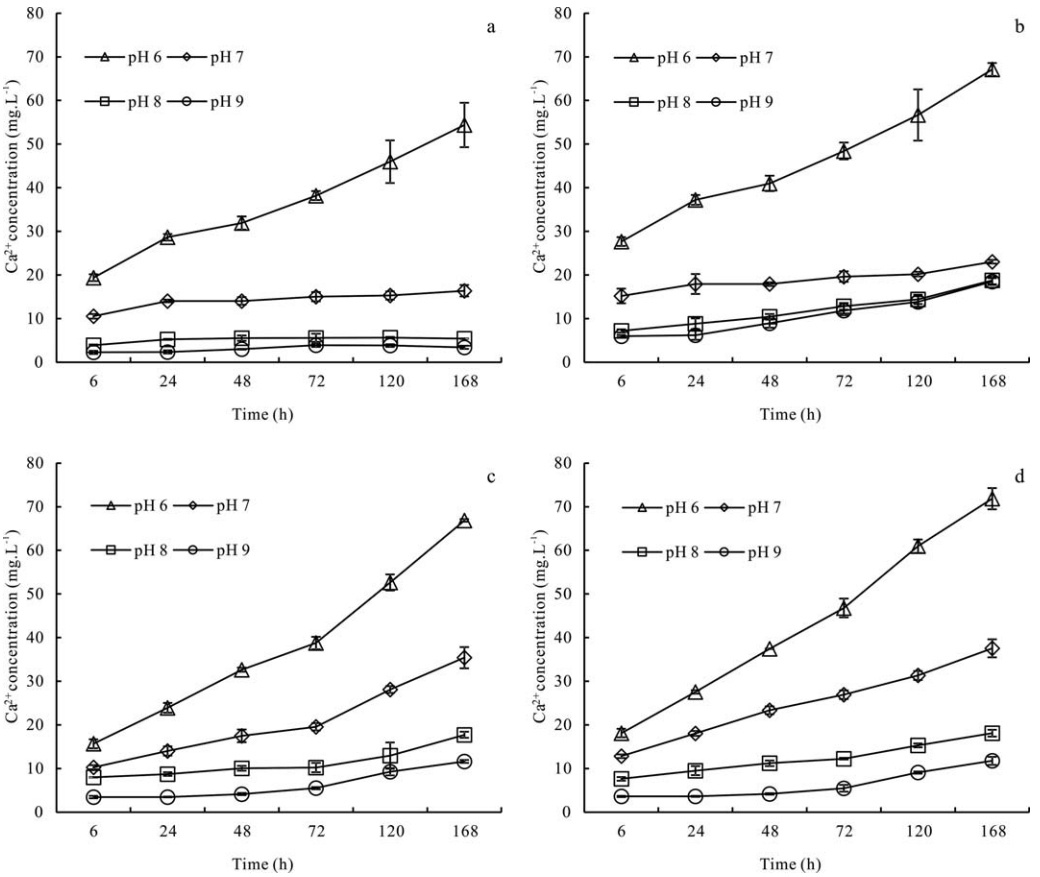

Figure 2. Concentrations of Ca^{2+} within the culture and algae body at different pH values after different hours of incubation ($mg{\cdot}L^{-1}$). (a) The treatment without microalgae (Control), (b) the treatment with *C. reinhardtii* (*C.R.*), (c) the treatment with *C. pyrenoidosa* (*C.P.*), and (d) the treatment with *M. aeruginosa* (*M.A.*). Error bars in Figures 2a–2d correspond to 1σ.

(Figure 3). For the treatments using *M.A.*, there was less increase at pH 6 than at pH 7–9 (Figure 3). After 72 h, there was less Mg^{2+} at pH 6 than at pH 7 for *M.A.* and *C.P.*, and there was less increase in the Mg^{2+} quantity than for treatments using *C.R.* (Figure 3).

The changes in Ca^{2+} and Mg^{2+} quantities over time differed from each other, suggesting that different mechanisms influenced these changes within the culture media and algae bodies.

3.3. Changes in Microalgal $\delta^{13}C$ and NPOC Under Different pH Values at Harvest

Microalgal $\delta^{13}C$ and NPOC values at different pH values are shown in Table 3. When pH increased, the NPOC also increased, but microalgal $\delta^{13}C$ values gradually decreased. The slow conversion between CO_2 and HCO_3^- produces approximately 10‰ $\delta^{13}C$ fractionation without catalysis, and the fractionation associated with the in vitro conversion catalyzed by carbonic anhydrase (CA) is 1.1‰ [*Marlier and O'Leary*, 1984; *Mook et al*., 1974]. The microalgae could convert more HCO_3^- into CO_2 for photosynthesis in treatments at higher pH, as these treatments contained higher proportions of HCO_3^-. The largest decrease was observed at pH values ranging from 8 to 9, and the proportion of HCO_3^- in this pH range was the largest among all the treatments. Meanwhile, the differences in microalgal $\delta^{13}C$ values under the same pH conditions but with the addition of different isotope-labeled calcites ($*\delta^{13}C_1$: calculated mean $\delta^{13}C$ value of $\delta^{13}C_1$ using equation (8) and $*\delta^{13}C_2$: calculated mean $\delta^{13}C$ value of $\delta^{13}C_2$ using equation (8)) decreased from 1.81‰ to 0.50‰, 1.39‰ to 0.46‰, and 1.96‰ to 0.42‰ for *C.R.*, *C.P.*, and *M.A.*, respectively, with increasing pH. This suggested that, as pH increased, the microalgae utilized more inorganic carbon from one source with a $\delta^{13}C$ value between the values obtained for the two added calcites (0.72‰ and −10.28‰, respectively). The mean $\delta^{13}C$ value for atmospheric CO_2 is approximately −7.8‰ [*Boutton*, 1991].

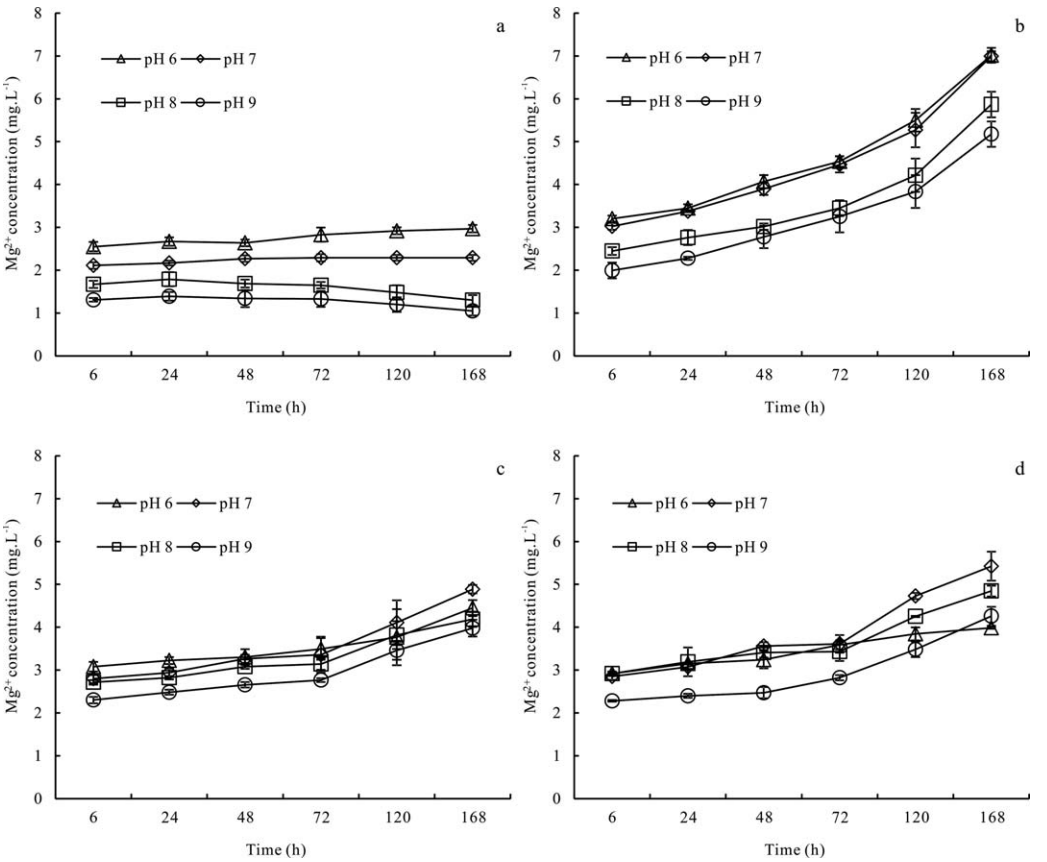

Figure 3. Concentrations of Mg^{2+} within the culture and algae body at different pH values after different hours of incubation ($mg{\cdot}L^{-1}$). (a) The treatment without microalgae (Control), (b) the treatment with *C. reinhardtii* (*C.R.*), (c) the treatment with *C. pyrenoidosa* (*C.P.*), and (d) the treatment with *M. aeruginosa* (*M.A.*). Error bars in Figures 3a–3d correspond to 1σ.

4. Discussion

4.1. Effect of pH on Calcite Biodissolution

The release of Ca^{2+} and Mg^{2+} is widely used to indicate carbonate dissolution [*Li et al.*, 2005; *Xiao et al.*, 2014]. However, unlike Ca^{2+}, Mg^{2+} has been identified as a limiting factor for algae growth under previous

Table 3. $\delta^{13}C$ Values of Microalgae Body and Concentration of NPOC at Harvest[a]

Microalgae	pH	$\delta^{13}C_1$ (‰)[b]	$NPOC_1$ (mg/L)[c]	$*\delta^{13}C_1$ (‰)[d]	$\delta^{13}C_2$ (‰)[e]	$NPOC_2$ (mg/L)	$*\delta^{13}C_2$ (‰)[f]
C.R	6	−16.05 ± 0.20	77.09 ± 3.05	−15.60 ± 0.22	−17.68 ± 0.25	67.64 ± 6.62	−17.41 ± 0.27
	7	−16.18 ± 0.25	73.04 ± 7.94	−15.72 ± 0.27	−17.70 ± 0.05	85.20 ± 8.48	−17.49 ± 0.05
	8	−16.94 ± 0.39	116.94 ± 3.22	−16.73 ± 0.44	−17.93 ± 0.14	124.19 ± 5.57	−17.81 ± 0.15
	9	−17.99 ± 0.17	119.66 ± 0.58	−17.87 ± 0.44	−18.45 ± 0.08	118.97 ± 8.71	−18.37 ± 0.08
C.P	6	−16.86 ± 0.29	109.38 ± 5.66	−16.40 ± 0.31	−18.11 ± 0.14	109.50 ± 9.18	−17.80 ± 0.15
	7	−17.01 ± 0.12	110.33 ± 11.99	−16.57 ± 0.13	−18.24 ± 0.61	103.60 ± 12.48	−17.92 ± 0.62
	8	−17.47 ± 0.03	128.51 ± 6.22	−17.15 ± 0.03	−18.29 ± 0.11	123.89 ± 11.27	−18.04 ± 0.11
	9	−18.76 ± 0.09	158.99 ± 7.65	−18.61 ± 0.09	−19.20 ± 0.22	154.03 ± 11.39	−19.07 ± 0.22
M.A	6	−16.05 ± 0.04	76.39 ± 13.58	−15.31 ± 0.04	−17.77 ± 0.23	70.65 ± 5.19	−17.2 5 ± 0.24
	7	−16.36 ± 0.29	88.77 ± 11.00	−15.78 ± 0.29	−18.05 ± 0.12	80.88 ± 4.63	−17.64 ± 0.12
	8	−17.07 ± 0.27	111.26 ± 17.09	−16.69 ± 0.27	−17.86 ± 0.05	102.10 ± 13.21	−17.53 ± 0.04
	9	−18.98 ± 0.20	119.46 ± 14.15	−18.81 ± 0.21	−19.36 ± 0.08	115.40 ± 6.51	−19.22 ± 0.08

[a]The $\delta^{13}C$ of microalgae body in treatments with *C. reinhardtii* (*C.R.*), *C. pyrenoidosa* (*C.P.*), and *M. aeruginosa* (*M.A.*) were measured using the method described in the section of calculation methods.
[b]$\delta^{13}C_1$: Measured mean (±1 SD) $\delta^{13}C$ value for the microalgae body in the treatment with calcite-1.
[c]NPOC: Mean (±1 SD) NPOC concentration.
[d]$*\delta^{13}C_1$: Calculated mean (±1 SD) $\delta^{13}C$ value of $\delta^{13}C_1$ using equation (8), i.e., the newborn algal $\delta^{13}C$.
[e]$\delta^{13}C_2$: Measured mean (±1 SD) $\delta^{13}C$ value for the microalgae body in the treatment with calcite-2.
[f]$*\delta^{13}C_2$: Calculated mean (±1 SD) $\delta^{13}C$ value of $\delta^{13}C_2$ using equation (8), i.e., the newborn algal $\delta^{13}C$.

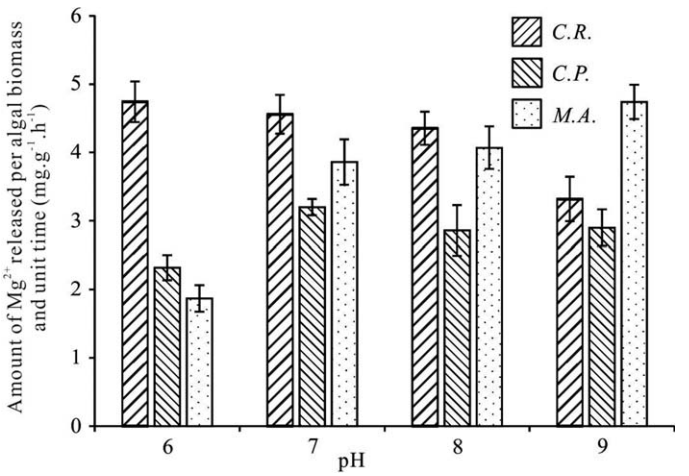

Figure 4. Amount of Mg^{2+} released per algal chlorophyll-a biomass and unit time (Pi) ($mg{\cdot}g^{-1}{\cdot}h^{-1}$) in treatments with *C. reinhardtii* (*C.R.*), *C. pyrenoidosa* (*C.P.*), and *M. aeruginosa* (*M.A.*) under different pH conditions. Error bars correspond to 1σ.

experimental conditions [*Xie and Wu*, 2014]. Moreover, Ca^{2+} is easily affected by $CaCO_3$ precipitation, and the amount of $CaCO_3$ precipitation is difficult to measure precisely. Therefore, in the current study, changes in Mg^{2+} quantities in culture media and algae bodies were used to indicate calcite dissolution.

The effects of pH on calcite chemical dissolution have been documented [*Chou et al*., 1989]. As shown in Figures 2 and 3, calcite chemical dissolution increased with decreasing pH, because the thermodynamic equilibrium of calcite dissolution ($Ca_xMg_{1-x}CO_3+CO_2+H_2O \leftrightarrow xCa^{2+}+(1-x)Mg^{2+}+2HCO_3^-$ or $Ca_xMg_{1-x}CO_3+H^+ \leftrightarrow xCa^{2+}+(1-x)Mg^{2+}+HCO_3^-$, $x \gg 1-x$) was strongly affected by pH. A body of water at low pH will have high levels of CO_2 and H^+. Therefore, calcite chemical dissolution is promoted at low pH. However, the release of Mg^{2+} caused by biological effects was not the same as that caused by chemical reactions alone. The amount of released Mg^{2+} at pH 6 was slightly higher than under other pH conditions and lower than at pH 7 and 8 after 72 h for both *M.A*. and *C.P*. (Figure 3). This result illustrates that the microalgae played a significant role in calcite dissolution and were strongly influenced by pH.

To assess how pH affects calcite biodissolution by microalgae, we constructed a model based on changes in biomass and biological action time (detailed description in 2.4.2. section). The biological cumulative action time model (supporting information Table S1) and Mg^{2+} released model (supporting information Table S2) was established.

As shown in Figure 4, the amount of released Mg^{2+} per unit algal biomass and unit time in *C.R*. decreased when the pH increased from 6 to 9. On the contrary, it increased with increasing pH for *M.A*. For *C.P*., it increased when the pH increased from 6 to 7, reached a maximum value, and then slightly decreased from pH 7 to 9. The different results were probably related to the different physiological characteristics of the microalgae, especially regarding inorganic carbon utilization. *C.R*. and *C.P*. can catalyze DIC transformation of HCO_3^- into CO_2 and increase CO_2 quantities through extracellular carbonic anhydrase (CAex) [*Aizawa and Miyachi*, 1986; *Williams and Turpin*, 1987]. Our previous studies found that the amounts of released Mg^{2+} per unit algal biomass and unit time in *C.R*. and *C.P*. under conditions of CAex inhibition were lower than under conditions without inhibition [*Xie and Wu*, 2014]. Other studies have also reported that bovine and microbial CAex can enhance the dissolution of carbonate minerals [*Li et al*., 2007; *Liu*, 2001]. Meanwhile, CAex activity is affected by pH. *Li et al*. [2012] showed that CAex activity in *Chlorella vulgaris* increases from pH 6.5 to 7.5 and reaches a peak enzyme activity of 18.6 $EU{\cdot}g^{-1}$, but this activity is completely inhibited from pH 7.5 to 9.5, reaching values as low as 11.3 $EU{\cdot}g^{-1}$. A similar trend was observed with the variation in Mg^{2+} release per unit algal biomass and unit time for *C.P*. We have also previously found that the CAex activities of *C.R*. and *C.P*. at pH 7.5 are clearly higher than those at pH 9.5 [*Wu et al*., 2011]. However, *M.A*. possesses no CAex activity and can only directly take up HCO_3^- under alkaline, CO_2-depleted conditions [*Aizawa and Miyachi*, 1986; *Bañares-España et al*., 2006; *Miller and Colman*, 1980]. Thus, at high pH values with a higher proportion of HCO_3^-, *M.A*. takes up more HCO_3^- as an inorganic carbon (Ci) source for photosynthesis through Na^+-dependent HCO_3^- transport as opposed to directly taking up more CO_2 at low pH [*Espie and Kandasamy*, 1994]. This behavior shifts the equation $Ca_xMg_{1-x}CO_3+CO_2+H_2O \leftrightarrow xCa^{2+}+(1-x)Mg^{2+}+2HCO_3^-$ toward dissolution. Other mechanisms may underlie the amount of Mg^{2+} that is released per unit algal biomass and unit time. Further research on this discovery is needed.

4.2. Effects of pH on $CaCO_3$ Reprecipitation

In Figure 3, it can be observed that the amounts of released Mg^{2+} in the treatments with microalgae were clearly higher than in those without microalgae. However, the difference in Ca^{2+} release between the treatments with and without microalgae was smaller (Figure 2). Therefore, the Ca^{2+} and Mg^{2+} concentrations were controlled by different mechanisms: Ca^{2+} may be strongly influenced by reprecipitation after being released from calcite because of the lower solubility of $CaCO_3$ (K^*_{sp}, $CaCO_3 = 4.8\times10^{-9}$ $mol \cdot L^{-1}$, $K = 298.15$ K) compared with $MgCO_3$ (K^*_{sp}, $MgCO_3 = 1\times10^{-5}$ $mol \cdot L^{-1}$, $K = 298.15$ K) [*Patnaik*, 2003]. Organic matter may be suitable for the formation of a secondary $CaCO_3$ precipitate at heterologous nucleation sites to consume Ca^{2+} produced from mineral dissolution in solution [*Xiao et al*., 2014]. When microalgae participate in a reaction, in addition to utilizing DIC, $CaCO_3$ precipitation can also be induced by "*Cis*" and "*Tran*" calcification mechanisms, which can change extracellular and intracellular microenvironments [*Heath et al*., 1995; *McConnaughey and Whelan*, 1997; *McConnaughey*, 1998; *Wang et al*., 2014].

Meanwhile, the ratio of the amount of released Ca^{2+} to the amount of released Mg^{2+} (71:1–60:1) was close to the mass ratio of Ca/Mg in calcite (66:1) in the treatment without microalgae at pH 6, which was virtually unaffected by chemical and biological precipitation (Figure 5). Therefore, we hypothesize that the main ion release mechanism is based on the intrinsic atomic ratios of calcite, and the amount of originally released Ca^{2+} can be deduced based on the amount of Mg^{2+} released from calcite.

The quantity of reprecipitated $CaCO_3$ can be obtained at harvest based on the theoretical quantity of Ca^{2+} released minus the actual measured quantity of Ca^{2+} released as follows:

$$W_{CaCO_3} = \left[N_{Mg} \cdot \left(m_{Ca}/m_{Mg}\right) - N_{Ca}\right] \cdot \left(m'_{CaCO_3}/m'_{Ca}\right) \tag{14}$$

where W_{CaCO_3} is the concentration of reprecipitated $CaCO_3$ ($mg \cdot L^{-1}$); N_{Mg} is the concentration of released Mg^{2+} ($mg \cdot L^{-1}$); N_{Ca} is the Ca^{2+} concentration in the system ($mg \cdot L^{-1}$); m_{Ca} and m_{Mg} are the Ca^{2+} and Mg^{2+} contents in calcite ($mg \cdot mg^{-1}$), respectively (Table 1); and m'_{CaCO_3} and m'_{Ca} are the molar masses of $CaCO_3$ and Ca^{2+} (g), respectively.

The greatest amount of reprecipitated $CaCO_3$ was found at pH 7 (Figure 6). When the pH increased, the amount of reprecipitated $CaCO_3$ decreased, probably because the amount of Ca^{2+} originally released at pH 7 was greater than at other pH conditions (8 and 9) (Figure 6). When a large amount of Ca^{2+} is released into water, more Ca^{2+} can be reprecipitated via chemical and biological actions. The least amount of reprecipitated $CaCO_3$ was found at pH 6 for both *C.P.* and *M.A.* (Figure 6). This maybe because the biodissolution was weaker and because the production of Ca^{2+} and HCO_3^- ions was smaller at pH 6 in both cases. CAex also has an important function in $CaCO_3$ precipitation [*Li et al*., 2013; *Xie and Wu*, 2014]. The different levels of CAex activity in the different microalgae species may also explain why the greatest amount of $CaCO_3$ precipitation was found for *C.R.*, which has the highest degree of CAex activity of the three species [*Aizawa and Miyachi*, 1986]. Meanwhile, the CAex activity of *C.P.* reached a maximum at pH 7, which was similar to the trend of $CaCO_3$ reprecipitation [*Li et al*., 2012]. CAex activity was not observed in *M.A.*, but this species has the ability to uptake HCO_3^- via transporters [*Pierce and Omata*, 1988]. *M.A.* exhibited the highest degree of growth at pH 7, at which

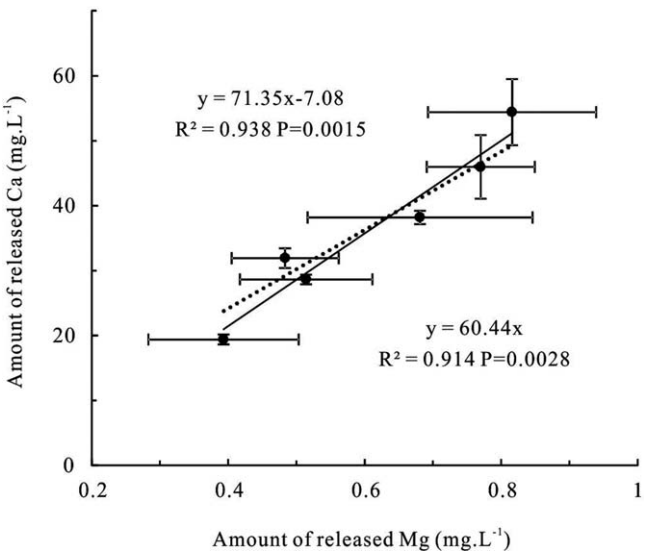

Figure 5. Amount of released Ca^{2+} versus amount of released Mg^{2+} in the treatment without microalgae at pH 6. The equation was fitted using SigmaPlot 10.0. The constant term was forced to return 0 in equation (y_2). Error bars correspond to 1σ.

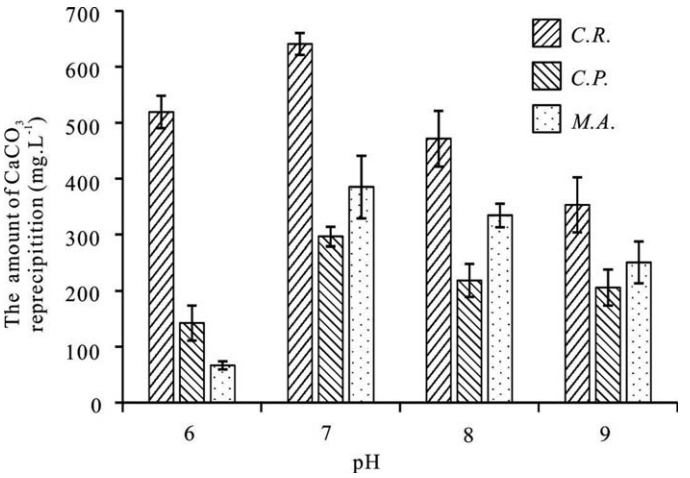

Figure 6. Reprecipitation amount of $CaCO_3$ in treatment with *C. reinhardtii* (*C.R.*), *C. pyrenoidosa* (*C.P.*), and *M. aeruginosa* (*M.A.*) under different pH conditions. Error bars correspond to 1σ.

this species could largely use calcification as a proton source to assimilate HCO_3^- for photosynthesis and nutrient acquisition [*McConnaughey and Whelan*, 1997].

4.3. Effects of pH on Microalgal DIC Utilization From Calcite Dissolution

In the current study, DIC, which was produced from the solubilization of atmospheric CO_2 and the dissolution of calcite, was taken up by the microalgae. The DIC originating from different sources had different $\delta^{13}C$ values. Thus, the microalgae that utilized different proportions of DIC from different sources displayed different $\delta^{13}C$ values (Table 3). Based on the differences in microalgae $\delta^{13}C$ values under the same treatment conditions but with different isotope-labeled calcites (0.72 ‰ and −10.29 ‰) and on the calculation model described in 2.4.4 section, the proportion of DIC utilized from calcite dissolution can be obtained (Figure 7).

The proportion of DIC utilized from calcite dissolution decreased with increasing pH (Figure 7) because the absolute amount of calcite dissolution was higher under low pH conditions than under high pH conditions (Figures 2 and 3). As such, the proportion of DIC from calcite dissolution in the medium was large at low pH as follows:

$$CaCO_3 + CO_2 + H_2O \leftrightarrow Ca^{2+} + 2HCO_3^- \tag{15}$$

The flux of atmospheric CO_2 to water is also controlled by pH as follows:

$$CO_2 \overset{k1}{\Longleftrightarrow} CO_2\ (aq) \text{ and } CO_2 + H_2O \overset{k2}{\Longleftrightarrow} HCO_3 + H^+ \tag{16}$$

$$K_2 = \frac{[HCO_3^-] \cdot [H^+]}{K_1 \cdot [CO_2(g)]} \tag{17}$$

$$Flux_{CO_2} = K \cdot \left(P_{CO_2 - atmosphere} - P_{CO_{2(g)}}\right) \tag{18}$$

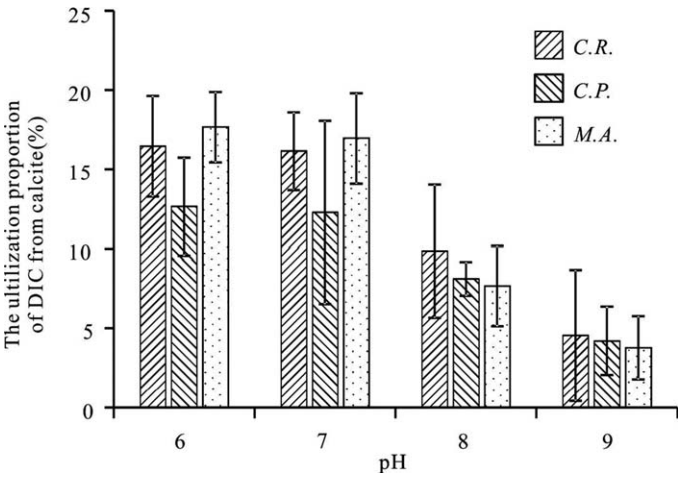

Figure 7. Proportion of DIC utilization from calcite dissolution (%) by *C. reinhardtii* (*C.R.*), *C. pyrenoidosa* (*C.P.*), and *M. aeruginosa* (*M.A.*) under different pH conditions. Error bars correspond to 1σ.

With decreasing pH, less CO_2 would come from the atmosphere within the medium, and the proportion of DIC from calcite dissolution would be reversed. The microalgae did not appear to selectively take up DIC from different sources. Thus, a low pH indicates a high proportion of DIC utilization from calcite dissolution. However, the three examined species of microalgae displayed unremarkable distinctions in their utilization proportions. Therefore, the different DIC compositions of the different sources were probably the main factor controlling the proportion of DIC utilization from calcite dissolution at different pH values.

4.4. Effects of pH on the CO_2 Sequestration in a Biokarst System

Each unit of calcite ($Ca_xMg_{1-x}CO_3$) dissolution absorbs a unit of CO_2 from the atmosphere to produce two units of HCO_3^-, as follows:

$$Ca_xMg_{1-x}{}^{**}CO_3 + {}^{*}CO_2 + H_2O \leftrightarrow xCa^{2+} + (1-x)Mg^{2+} + H^{**}CO_3^- + H^{*}CO_3^- \quad (19)$$

$H^{**}CO_3^-$ and $H^{*}CO_3^-$ go through the same pathway because they possess the same physical and chemical properties (**C: the carbon from calcite; *C: the carbon from CO_2). Thus, equation (19) can be transformed into

$$Ca_xMg_{1-x}CO_3 + CO_2 + H_2O \leftrightarrow xCa^{2+} + (1-x)Mg^{2+} + 2HCO_3^- \quad (20)$$

This process takes place in the absence of photosynthetic organisms. Once the participation of photosynthetic organisms is included, the process becomes more interesting and complex, namely biokarst. Portions of the HCO_3^- and Ca^{2+} may be involved in the physiological processes of microalgae, as follows:

$$yCa^{2+} + 2yHCO_3^- + aH_2O \rightarrow a(CH_2O + O_2) + (y-0.5a)(CaCO_3 + CO_2 + H_2O) + (0.5a-ab)Ca^{2+} + aOH^- \quad (21)$$

The carbon in HCO_3^- is converted into three forms, namely, organic matter (CH_2O) formed via microalgal photosynthesis, $CaCO_3$ precipitate, and residue in water, as detailed in Figure 8.

Therefore, the amount of carbon in the form of HCO_3^- ($H^{**}CO_3^-$ and $H^{*}CO_3^-$) following calcite dissolution (***M) can be expressed as follows:

$${}^{***}M = M_{CH_2O} + M_{HCO_3^-} + (M_{CaCO_3} + M_{CO_2}) \quad (22)$$

where M_{CH_2O} is the amount of carbon from HCO_3^- converted into organic matter via microalgal photosynthesis; $M_{HCO_3^-}$ is the amount of HCO_3^- residue in water; and $(M_{CaCO_3} + M_{CO_2})$ is the amount of carbon from HCO_3^- that reprecipitated to form $CaCO_3$ and released the equivalent amount of CO_2, as $M_{CaCO_3} = M_{CO_2}$. Thus, the equation can be transformed as follows:

$${}^{***}M = M_{CH_2O} + M_{HCO_3^-} + 2M_{CaCO_3} = M_{CH_2O} + M_{HCO_3^-} + 2M_{CO_2} \quad (23)$$

where ***M can be estimated by the amount of released Mg^{2+} from calcite dissolution as follows:

$${}^{***}M = 2N_{Mg} \cdot \left(\frac{m_C}{m_{Mg}}\right) \quad (24)$$

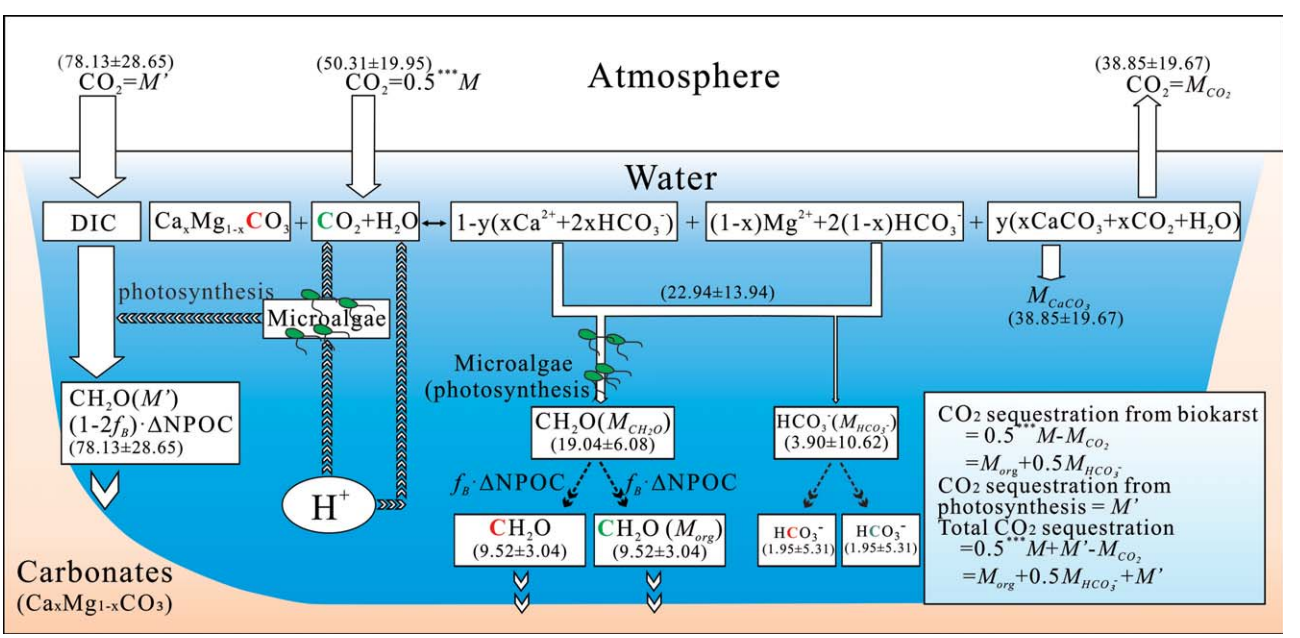

Figure 8. Schematic of carbon transport processes and average value of different pH conditions (mg·L^{-1}) between different carbon pools in the biokarst system.

where N_{Mg} is the concentration of Mg^{2+} released from calcite ($mg \cdot L^{-1}$); m_C is the carbon content in calcite ($g \cdot g^{-1}$); and m_{Mg} is the Mg^{2+} content in calcite ($g \cdot g^{-1}$).

M_{CH2O} can be determined based on the proportion of inorganic carbon utilization from calcite (f_B, %) and the increase in NPOC over the entire cultivation process (△NPOC, $mg \cdot L^{-1}$) (detailed description in 2.4.4. section) as follows:

$$M_{CH_2O} = 2f_B \cdot \Delta\mathrm{NPOC} \tag{25}$$

M_{CaCO3} can be obtained based on the Ca^{2+} concentration in the system, the amount of released Mg^{2+}, and the mass ratio of Ca/Mg in calcite as follows:

$$M_{CaCO_3} = \left[N_{Mg} \cdot \left(\frac{m_{Ca}}{m_{Mg}}\right) - N_{Ca}\right] \cdot \left(\frac{m'_C}{m'_{Ca}}\right) \tag{26}$$

N_{Mg} is the amount of released Mg^{2+} ($mg \cdot L^{-1}$); N_{Ca} is the Ca^{2+} concentration in the system ($mg \cdot L^{-1}$); m_{Ca} and m_{Mg} are the Ca^{2+} and Mg^{2+} contents in calcite ($mg \cdot mg^{-1}$), respectively (Table 1), and m'_C and m'_{Ca} are the C and Ca^{2+} contents in $CaCO_3$ ($g \cdot g^{-1}$), respectively.

The three pathways available for HCO_3^- produce different CO_2 sequestration abilities. The $CaCO_3$ precipitation process releases an equivalent amount of CO_2. Thus, it would not produce a carbon sink. Only half of the carbon in M_{CH_2O} and $M_{HCO_3^-}$ comes from atmospheric CO_2; the other half came from calcite. Therefore, the amount (*M) of CO_2 sequestration from the atmosphere, which is related to the calcite dissolution in the system, can be expressed using the following equation:

$$^*M = 0.5M_{CH_2O} + 0.5M_{HCO_3^-} = M_{org} + 0.5M_{HCO_3^-} = 0.5^{***}M - M_{CO_2} \tag{27}$$

Moreover, in the interaction between microalgae and calcite, microalgae can also directly utilize DIC derived from water-atmospheric CO_2 exchange, which does not depend on calcite dissolution. The amount of CO_2 can be obtained through the increase in NPOC over the entire cultivation process (△NPOC, $mg \cdot L^{-1}$) and the proportion of inorganic carbon utilization from calcite (f_B, %) as follows:

$$M\prime = \Delta NPOC - 2f_B \cdot \Delta NPOC \tag{28}$$

Therefore, the total CO_2 sequestration amount (M) includes two parts: the first is the CO_2 sequestration related to calcite dissolution, which can be called the biokarst carbon sink (*M), and the second is produced from the direct utilization of DIC by microalgae via water-atmospheric CO_2 exchange, which can be called the photosynthetic carbon sink (M'), as follows:

$$M = {}^*M + M' \tag{29}$$

Finally, the total carbon sink, in addition to the different forms of carbon in the biokarst system can be obtained (Table 4).

The biokarst carbon sink (*M) increased with decreasing pH (Table 4) because the rate of calcite dissolution to $CaCO_3$ reprecipitation was greater at low pH. Thus, the amount of atmospheric CO_2 that was consumed and turned into HCO_3^- in water via carbonate dissolution increased with decreasing pH. One part of this DIC can be taken up and further turned into organic matter (M_{org}) by microalgae. The amount decreased when the pH increased above 7. At pH 6, although the proportion of DIC utilized by the microalgae from calcite dissolution was the highest (Figure 7), the organic carbon synthetic ability of the microalgae was the weakest (Table 3). The other part of HCO_3^- was present as residue in the water ($M_{HCO_3^-}$). The amount of residual HCO_3^- ($M_{HCO_3^-}$) generally decreased with increasing pH. However, the values were negative in particular cases. This illustrated that the process of $CaCO_3$ reprecipitation releases a larger amount of CO_2 ($Ca^{2+} + 2HCO_3^- \leftrightarrow CaCO_3 + CO_2 + H_2O$) than does residual HCO_3^- from calcite dissolution after uptake by microalgae. Thus, it is widely accepted that the weathering of carbonate rocks does not represent an important carbon sink over a long-term timescale because all of the CO_2 that is consumed in calcite dissolution is returned to the atmosphere by the relatively rapid precipitation of carbonates ($Ca^{2+} + 2HCO_3^- \leftrightarrow CaCO_3 + CO_2 + H_2O$), assuming aquatic photosynthesis is not considered [*Berner et al.*, 1983; *Elderfield*, 2010]. However, the uptake of CO_2 consumed during carbonate dissolution via aquatic photosynthesis effectively prevents it from being returned to the atmosphere via carbonate precipitation, especially at $pH < 9$. When the biotic degradation and photochemical reactions are considered, this organic carbon from microalgae may be remineralized and returned to the atmosphere during transport. The

Table 4. Carbon Sink From Different Processes in the Biokarst System[a]

Microalgae	pH	Carbon Sink Originating From the Dissolution of Calcite (*M) (mg·L^{-1})			Carbon sink Originated From Directly Utilization (M')[e] (mg·L^{-1})	Total Carbon Sink (M)[f] (mg·L^{-1})
		$M_{HCO_3^-}$[b]	M_{org}[c]	*M[d]		
C.R.	6	11.56 ± 2.60	11.19 ± 2.21	22.75 ± 3.42	45.65 ± 5.39	68.39 ± 6.38
	7	−0.66 ± 4.00	10.33 ± 2.03	9.67 ± 4.48	43.32 ± 8.92	52.99 ± 9.98
	8	−3.07 ± 4.66	10.63 ± 4.52	7.56 ± 6.50	86.61 ± 9.61	94.17 ± 11.60
	9	1.82 ± 7.64	5.03 ± 4.55	6.85 ± 8.89	100.52 ± 9.12	107.38 ± 12.74
C.P.	6	8.80 ± 740	12.38 ± 3.09	21.18 ± 8.03	73.08 ± 8.39	94.26 ± 11.61
	7	−0.07 ± 7.72	12.14 ± 5.89	12.07 ± 9.71	74.51 ± 16.82	86.59 ± 19.42
	8	−3.28 ± 3.14	9.49 ± 1.34	6.21 ± 3.41	97.99 ± 6.78	104.20 ± 7.59
	9	−1.95 ± 3.47	6.21 ± 3.19	4.25 ± 4.72	135.04 ± 9.97	139.30 ± 11.03
M.A.	6	10.80 ± 2.94	11.66 ± 2.81	22.46 ± 4.07	42.71 ± 14.70	65.17 ± 15.25
	7	−0.08 ± 5.50	13.29 ± 2.92	13.21 ± 6.23	51.84 ± 12.45	65.05 ± 13.92
	8	−0.87 ± 4.12	7.73 ± 2.87	6.86 ± 5.02	85.45 ± 18.03	92.31 ± 18.71
	9	0.39 ± 4.87	4.12 ± 2.24	4.51 ± 5.36	100.86 ± 14.84	105.37 ± 15.78
Average		1.95 ± 5.31	9.52 ± 3.04	11.47 ± 6.97	78.13 ± 28.65	89.60 ± 23.92

[a]Carbon sink from different processes and in different forms in treatments with *C. reinhardtii* (*C.R.*), *C. pyrenoidosa* (*C.P.*), and *M. aeruginosa* (*M.A.*) were calculated using the equations (22–29).
[b]$M_{HCO_3^-}$: Absorbed atmosphere carbon caused by calcite dissolution and then residue in water.
[c]M_{org}: Absorbed atmosphere carbon caused by calcite dissolution and then further utilized by microalgae.
[d]*M: Total absorbed atmosphere carbon caused by calcite dissolution (Karst carbon sink).
[e]M': Absorbed atmosphere carbon due to directly taken up by the microalgae (Photosynthetic carbon sink).
[f]M: Absorbed atmosphere carbon in the system (Total carbon sink).

global CO_2 emission from lakes is 0.53 Pg C·yr^{-1} due to mineralization resulting in CO_2 supersaturation, taking into account the various lake types as well as recent estimates of the global area of lakes [*Tranvik et al*., 2009]. *Jonsson et al*. [2001] estimated the primary production contributed approximately 20% of the remineralization of organic carbon in a lake in northern Sweden. If we used the global gross primary production (GPP) of lakes (0.65 Pg C·yr^{-1}) to make a rough estimation, there remains approximately 0.54 Pg C·yr^{-1} of organic carbon from GPP buried in sediment or transported to the ocean [*Pace and Prairie*, 2005]. Sedimentary carbon often accumulates over thousands of years and represents a long-term carbon sink [*Einsele et al*., 2001; *Tranvik et al*., 2009]. The organic carbon entering the ocean may be decomposed into DIC while being vertical transported into deep-sea sediment, but these DIC in deep sea water will travel with the great ocean conveyor system in thousands of years timescale (<3ka) [*Broecker*, 1991]. Therefore, based on these results, the atmospheric CO_2 sink associated with carbonate weathering cannot be neglected when considering the global carbon cycle on the timescale of thousands of years if aquatic photosynthesis is involved. Although the thousands of years timescale of the carbon sink associated with carbonate weathering is much shorter than the 50–100 Ma timescale of Ca-silicate chemical weathering and subsequent deposition as carbonate in the oceans, it is essential for changes in atmospheric CO_2 over human history [*Bickle*, 1996]. The reaction between H^+ and $CaCO_3$ follows a first-order reaction pattern, and the relationship between the concentration of H^+ and pH follows a negative exponential pattern. Thus, we choose a negative exponential function to simulate a correlation between pH and the biokarst carbon sink. If we choose pH 8 as the reference for a karstic lake and build a correlation between pH and karst carbon sink change, we roughly obtain the variation in the biokarst carbon sink with pH (supporting information Figure S1), as follows:

$$^{*}M(\%) = 0.51 + 387e^{-0.83pH} \quad \left(R^2 = 0.96,\ n = 12,\ P < 0.0001\right) \tag{30}$$

In this system, microalgae can also directly utilize DIC from water-atmospheric CO_2 exchange to produce a photosynthetic carbon sink (M'), which increased with increasing pH (Table 4). This result may be attributed to the fact that the atmospheric CO_2 flux into water was larger at higher pH versus the smaller quantity of DIC produced from calcite dissolution at high pH, as shown in equations (16), (17), and (18). Moreover, the total photosynthetic organic carbon ($M' + M_{org}$) also increased with increasing pH (Tables 3 and 4). *Khalil* et al. [2010] also found that pigment content decreases and dry weight and carbohydrate content increase in *Chlorella ellipsoidea* when pH increases from 6 to 9. RUBISCO-containing pyrenoid and carbohydrates have been speculated to function as sites of CO_2 evolution in *C. reinhardtii* at high pH when the concentration of HCO_3^- increases [*Sültemeyer et al*., 1995]. The thylakoid inclusions in the pyrenoid may be enhanced to create a large proton concentration for green algal and cyanobacterial photosynthetic symbionts, which

could help facilitate the conversion of HCO_3^- into CO_2 [*Badger et al.*, 1993]. Thus, microalgae may improve the production of functional pyrenoid and carbohydrates to increase NPOC at high pH. Similarly, the reaction between H^+ and HCO_3^- ($CO_2+H_2O \leftrightarrow H^+ + HCO_3^-$), a rate-limiting step in algal photosynthesis, which directly affects the CO_2 flux, also follows first-order reaction patterns. Thus, we can build a exponential function to simulate the correlation between pH and changes in the photosynthetic carbon sink relative to pH 8 (supporting information Figure S1):

$$M'(\%) = 0.21 + 0.04e^{0.37pH} \quad \left(R^2 = 0.86,\ \ n = 12,\ \ P = 0.0002\right) \tag{31}$$

The total carbon sink (M) increased with increasing pH above pH 7 (Table 4). With increasing pH, the karst carbon sink ($*M$) decreased, but the larger magnitude photosynthetic carbon sink (M') increased. The photosynthetic carbon sink (M') was 2–28 times greater than the karst carbon sink ($*M$) under different pH values (from 6 to 9) for the three microalgae species. This result indicates that the biokarst system ($CaCO_3$-CO_2-microalgae) produces a minimum carbon sink at a specific pH then increases with increasing pH. When we synthetically consider the two types of carbon sinks, we get a correlation between the variation in the total carbon sink and the variation in pH:

$$M(\%) = \left(25.63 + 3062e^{-0.85pH} + 2.79e^{0.39pH}\right)/97 \tag{32}$$

The acidification of lakes caused by anthropogenic activities, such as acid mine drainage, acidic atmospheric deposition, and other factors, has been widespread since the Industrial Revolution [*Battarbee et al.*, 1985; *Rice and Herman*, 2012]. If karst lakes decrease by one pH unit relative to pH 8, the biokarst carbon sink at pH 7 will be 167% greater than that at pH 8. Moreover, karst lakes also appear to exhibit natural seasonal changes in pH. The pH ranged from 7.1 to nearly 10.3 in the surface of Esthwaite Water, Cumbria (54″22′N, 2′59′W) [*Maberly*, 1996]. If we choose an average local pH value (7.6) as the reference pH, we can estimate that the variations in the karst carbon sink, photosynthetic carbon sink, and total carbon sink are 48%–130%, 87%–232%, and 92%–214%, respectively. Therefore, the biokarst ($CaCO_3$-CO_2-microalgae) system is important for atmospheric CO_2 sequestration and is very sensitive to pH changes.

5. Conclusions

The pH of the water was found to play an important role in three key microalgal biokarst processes, including calcite dissolution, $CaCO_3$ reprecipitation, and inorganic carbon assimilation. Calcite dissolution decreased when the pH increased from 6 to 9. For biodissolution, it decreased when the pH increased from 6 to 9 for *C.R*. On the contrary, it increased when the pH increased for *M.A*. For *C.P*., it increased when the pH increased from 6 to 7, reached a maximum, and then slightly decreased as the pH dropped from 7 to 9. $CaCO_3$ reprecipitation and DIC utilization by microalgae from calcite dissolution decreased when the pH increased from 7 to 9.

The dissolution of calcite consumes atmospheric CO_2; however, the consumed CO_2 is either utilized by microalgae to form organic carbon, released back into the atmosphere because of $CaCO_3$ reprecipitation, or remains as a residue in water. Every process examined above had different CO_2 sequestration abilities. The CO_2 sequestration produced from calcite dissolution, including carbon utilization by microalgae and carbon residue in water, decreased when the pH increased from 6 to 9. However, the CO_2 directly absorbed from the atmosphere via microalgal photosynthesis increased when the pH increased from 6 to 9. Based on the above-mentioned results, in the biokarst system ($CaCO_3$-CO_2-microalgae), the photosynthetic carbon sink decreases with decreasing pH, and the biokarst carbon sink behaves oppositely within the range from pH 6 to 9. Therefore, the total carbon sink shows a minimum at a specific pH then increases with decreasing pH. Therefore, biokarst plays an important role in providing a negative feedback on the release of CO_2 due to a decrease in pH and is an unneglectable carbon sink process on a timescale of thousands of years (<3 ka).

Acknowledgments
The study was supported by National Key Basic Research Program of China (2013CB956701), and the National Key Research and development Program of China (2016YFC0502602). Data can be made available upon request to the corresponding author (wuyanyou@mail.gyig.ac.cn).

References

Aizawa, K., and S. Miyachi (1986), Carbonic anhydrase and CO_2 concentrating mechanisms in microalgae and cyanobacteria, *FEMS. Microbiol. Lett.*, *39*(3), 215–233, doi:10.1016/0378-1097(86)90447-7.

Azov, Y. (1982), Effect of pH on inorganic carbon uptake in algal cultures, *Appl. Environ. Microbiol.*, *43*(6), 1300–1306.

Badger, M. R., H. Pfanz, B. Büdel, U. Heber, and O. L. Lange (1993), Evidence for the functioning of photosynthetic CO_2-concentrating mechanisms in lichens containing green algal and cyanobacterial photobionts, *Planta*, *191*(1), 57–70, doi:10.1007/BF00240896.

Bañares-España, E., V. López-Rodas, C. Salgado, E. Costas, and A. Flores-Moya (2006), Inter-strain variability in the photosynthetic use of inorganic carbon, exemplified by the pH compensation point, in the cyanobacterium *Microcystis aeruginosa*, *Aquat. Bot.*, *85*(2), 159–162, doi:10.1016/j.aquabot.2006.03.009.

Battarbee, R. W., R. J. Flower, A. C. Stevenson, and B. Rippey (1985), Lake acidification in Galloway: A palaeoecological test of competing hypotheses, *Nature*, *314*(28), 350–352, doi:10.1038/314350a0.

Berner, R. A., A. C. Lasaga, and R. M. Garrels (1983), The carbonate-silicate geochemical cycle and its effect on atmospheric carbon dioxide over the past 100 million years, *Am. J. Sci.*, *283*(7), 641–683, doi:10.2475/ajs.283.7.641.

Bickle, M. (1996), Metamorphic decarbonation, silicate weathering and the long-term carbon cycle, *Terra Nova*, *8*(3), 270–276.

Boschker, H., and J. Middelburg (2002), Stable isotopes and biomarkers in microbial ecology, *FEMS. Microbiol. Ecol.*, *40*(2), 85–95, doi: 10.1111/j.1574-6941.2002.tb00940.x.

Boutton, T. W. (1991), Stable carbon isotope ratios of natural materials: I. Sample preparation and mass spectrometric analysis, in *Carbon Isotope Techniques*, edited by D. C. Coleman, B. Fry, pp. 155–171, Academic, San Diego, New York.

Broecker, W. S. (1991), The great ocean conveyor, *Oceanography*, *4*(2), 79–89, doi:10.5670/oceanog.1991.07.

Buchanan, D., and B. Corcoran (1959), Sealed Tube Combustions for Determination of Carbon-14 and Total Carbon, *Anal. Chem.*, *31*(10), 1635–1638.

Chen, Z., H. Cheng, and X. Chen (2009), Effect of Cl^- on photosynthetic bicarbonate uptake in two cyanobacteria *Microcystis aeruginosa* and *Synechocystis* PCC6803, *Chin. Sci. Bull.*, *54*(7), 1197–1203, doi:10.1007/s11434-009-0148-9.

Chetelat, B., C.-Q. Liu, Z. Zhao, Q. Wang, S. Li, J. Li, and B. Wang (2008), Geochemistry of the dissolved load of the Changjiang Basin rivers: Anthropogenic impacts and chemical weathering, *Geochim. Cosmochim. Acta*, *72*(17), 4254–4277, doi:10.1016/j.gca.2008.06.013.

Chou, L., R. M. Garrels, and R. Wollast (1989), Comparative study of the kinetics and mechanisms of dissolution of carbonate minerals, *Chem. Geol.*, *78*(3), 269–282, doi:10.1016/0009-2541(89)90063-6.

Elderfield, H. (2010), Seawater chemistry and climate, *Science*, *327*(5969), 1092–1093, doi:10.1126/science.1186769.

Einsele, G., J. Yan, and M. Hinderer (2001), Atmospheric carbon burial in modern lake basins and its significance for the global carbon budget, *Global Planet. Change*, *30*(3), 167–195.

Espie, G. S., and R. A. Kandasamy (1994), Monensin inhibition of Na^+-dependent HCO_3^- transport distinguishes it from Na^+-independent HCO_3^- transport and provides evidence for Na^+/HCO_3^- symport in the cyanobacterium *Synechococcus* UTEX 625. *Plant Physiol.*, *104*(4), 1419–1428, doi:10.1104/pp.104.4.1419.

Gombert, P. (2002), Role of karstic dissolution in global carbon cycle, *Global Planet. Change*, *33*(1), 177–184, doi:10.1016/S0921-8181(02)00069-3.

Han, G., Y. Tang, and Z. Xu (2010), Fluvial geochemistry of rivers draining karst terrain in Southwest China, *J. Asian Earth Sci.*, *38*(1), 65–75.

Heath, C. R., B. C. Leadbeater and M. E. Callow (1995), Effect of inhibitors on calcium carbonate deposition mediated by freshwater algae. *J. Appl. Phycol.*, *7*(4) 367–380, doi:10.1007/BF00003794.

Huang, C. Y. L., and E. Schulte (1985), Digestion of plant tissue for analysis by ICP emission spectroscopy, *Commun. Soil. Sci. Plant. Anal.*, *16*(9), 943–958, doi:10.1080/00103628509367657.

Huang, T.-L., and H.-B. Cong (2007), A new method for determination of chlorophylls in freshwater algae, *Environ. Monit. Assess.*, *129*(1-3), 1–7, doi:10.1007/s10661-006-9419-y.

Jonsson, A., M. Meili, A.-K. Bergström, and M. Jansson (2001), Whole-lake mineralization of allochthonous and autochthonous organic carbon in a large humic lake (Örträsket, N. Sweden), *Limnol. Oceanogr.*, *46*(7), 1691–1700.

Khalil, Z. I., M. M. Asker, S. El-Sayed, and I. A. Kobbia (2010), Effect of pH on growth and biochemical responses of *Dunaliella bardawil* and *Chlorella ellipsoidea*. *World. J. Microbiol. Biotechnol.*, *26*(7), 1225–1231, doi:10.1007/s11274-009-0292-z.

Kump, L. R., S. L. Brantley, and M. A. Arthur (2000), Chemical Weathering, Atmospheric CO2, and Climate, *Annu. Rev. Earth Planet. Sci.*, *28*(1), 611–667, doi: 10.1146/annurev.earth.28.1.611.

Lerman, A., and F. T. Mackenzie (2005), CO_2 air–sea exchange due to calcium carbonate and organic matter storage, and its implications for the global carbon cycle, *Aquat. Geochem.*, *11*(4), 345–390, doi:10.1007/s10498-005-8620-x.

Li, L., M. L. Fu, Y. H. Zhao, and Y. T. Zhu (2012), Characterization of carbonic anhydrase II from *Chlorella vulgaris* in bio-CO_2 capture, *Environ. Sci. Pollut. Res. Int.*, *19*(9), 4227–4232, doi:10.1007/s11356-012-1077-8.

Li, W., L.-j. Yu, Q.-f. He, Y. Wu, D.-x. Yuan, and J.-h. Cao (2005), Effects of microbes and their carbonic anhydrase on Ca^{2+} and Mg^{2+} migration in column-built leached soil-limestone karst systems, *Appl. Soil Ecol.*, *29*(3), 274–281, doi:10.1016/j.apsoil.2004.12.001.

Li, W., L. J. Yu, Y. Wu, L. P. Jia, and D. X. Yuan (2007), Enhancement of Ca^{2+} release from limestone by microbial extracellular carbonic anhydrase, *Bioresour. Technol.*, *98*(4), 950–953, doi:10.1016/j.biortech.2006.03.021.

Li, W., W.-S. Chen, P.-P. Zhou, L. Cao, and L.-J. Yu (2013), Influence of initial pH on the precipitation and crystal morphology of calcium carbonate induced by microbial carbonic anhydrase, *Colloids Surf. B*, *102*, 281–287, doi:10.1016/j.colsurfb.2012.08.042.

Liu, Z. (2001), Role of carbonic anhydrase as an activator in carbonate rock dissolution and its implication for atmospheric CO_2 sink, *Acta Geol. Sin. [English ed.]*, *75*(3), 275–278, doi:10.1111/j.1755-6724.2001.tb00531.x.

Liu, Z., W. Dreybrodt, and H. Wang (2010), A new direction in effective accounting for the atmospheric CO_2 budget: Considering the combined action of carbonate dissolution, the global water cycle and photosynthetic uptake of DIC by aquatic organisms, *Earth Sci. Rev.*, *99*(3-4), 162–172, doi:10.1016/j.earscirev.2010.03.001.

Liu, Z., W. Dreybrodt, and H. Liu (2011), Atmospheric CO_2 sink: Silicate weathering or carbonate weathering?, *Appl. Geochem.*, *26*, S292–S294, doi:10.1016/j.apgeochem.2011.03.085.

Maberly, S. (1996), Diel, episodic and seasonal changes in pH and concentrations of inorganic carbon in a productive lake, *Freshwater Biol.*, *35*(3), 579–598, doi:10.1111/j.1365-2427.1996.tb01770.x.

Marlier, J. F., and M. H. O'Leary (1984), Carbon kinetic isotope effects on the hydration of carbon dioxide and the dehydration of bicarbonate ion, *J. Am. Chem. Soc.*, *106*(18), 5054–5057, doi:10.1021/ja00330a003.

McConnaughey, T. (1998), Acid secretion, calcification, and photosynthetic carbon concentrating mechanisms, *Can. J. Bot.*, *76*(6), 1119–1126, doi:10.1139/b98-066.

McConnaughey, T., and J. Whelan (1997), Calcification generates protons for nutrient and bicarbonate uptake, *Earth Sci. Rev.*, *42*(1), 95–117, doi:10.1016/S0012-8252(96)00036-0.

McCrea, J. M. (1950), On the isotopic chemistry of carbonates and a paleotemperature scale, *J. Chem. Phys.*, *18*(6), 849–857, doi:10.1063/1.1747785.

Menéndez, M., M. Martínez, and F. A. Comín (2001), A comparative study of the effect of pH and inorganic carbon resources on the photosynthesis of three floating macroalgae species of a Mediterranean coastal lagoon, *J. Exp. Mar. Biol. Ecol.*, *256*(1), 123–136, doi:10.1016/S0022-0981(00)00313-0.

Meybeck, M. (1993), Riverine transport of atmospheric carbon: sources, global typology and budget, *Water, Air, Soil Pollut.*, *70*(1–4), 443–463, doi:10.1007/BF01105015.

Miller, A. G., and B. Colman (1980), Evidence for HCO_3^- transport by the blue-green algae (*cyanobacterium*) *Coccochloris peniocystis*, *Plant Physiol.*, *65*(2), 397–402, doi:10.1104/pp.65.2.397.

Mook, W., J. Bommerson, and W. Staverman (1974), Carbon isotope fractionation between dissolved bicarbonate and gaseous carbon dioxide, *Earth Planet Sc. Lett.*, *22*(2), 169–176, doi:10.1016/0012-821.

Pace, M. L., and Y. T. Prairie (2005), Respiration in lakes, in *Respiration in Aquatic Ecosystems*, edited by P. A. del Giorgio and P. J. l. B. Williams, pp. 103–121, Oxford Univ. Press, New York.

Patnaik, P. (2003), *Handbook of Inorganic Chemicals*, McGraw-Hill, New York.

Pierce, J., and T. Omata (1988), Uptake and utilization of inorganic carbon by cyanobacteria, *Photosynth. Res.*, *16*(1-2), 141–154, doi:10.1007/BF00039490.

Plummer, L. N., and T. Wigley (1976), The dissolution of calcite in CO_2-saturated solutions at 25°C and 1 atmosphere total pressure, *Geochim. Cosmochim. Acta*, *40*(2), 191–202, doi:10.1016/0016-7037(76)90176-9.

Radajewski, S., P. Ineson, N. R. Parekh, and J. C. Murrell (2000), Stable-isotope probing as a tool in microbial ecology, *Nature*, *403*(6770), 646–649, doi:10.1038/35001054.

Rice, K. C., and J. S. Herman (2012), Acidification of Earth: An assessment across mechanisms and scales, *Appl. Geochem.*, *27*(1), 1–14, doi:10.1016/j.apgeochem.2011.09.001.

Sültemeyer, D., G. Amoroso, and H. Fock (1995), Induction of intracellular carbonic anhydrases during the adaptation to low inorganic carbon concentrations in wild-type and ca-1 mutant cells of *Chlamydomonas reinhardtii*, *Planta*, *196*(2), 217–224, doi:10.1007/BF00201377.

Taylor, G., P. Trudinger, and D. Swine (1979), *Biogeochemical Cycling of Mineral-Forming Elements*, Elsevier, New York.

Topper, K., and J. Kotuby-Amacher (1990), Evaluation of a closed vessel acid digestion method for plant analyses using inductively coupled plasma spectrometry, *Commun. Soil. Sci. Plant. Anal.*, *21*(13–16), 1437–1455, doi:10.1080/00103629009368315.

Tranvik, L. J., J. A. Downing, J. B. Cotner, S. A. Loiselle, R. G. Striegl, T. J. Ballatore, P. Dillon, K. Finlay, K. Fortino, and L. B. Knoll (2009), Lakes and reservoirs as regulators of carbon cycling and climate, *Limnol. Oceanogr.*, *54*(6part2), 2298–2314.

Vörös, L., and J. Padisák (1991), Phytoplankton biomass and chlorophyll-a in some shallow lakes in central Europe, *Hydrobiologia*, *215*(2), 111–119, doi:10.1007/BF00014715.

Wang, P., Q. Hu, H. Yang, J. Cao, L. Li, Y. Liang, and K. Wang (2014), Preliminary study on the utilization of Ca^{2+} and HCO_3^- in karst water by different sources of *Chlorella vulgaris*, *Carbonate Evaporite*, *29*(2), 203–210, doi:10.1007/s13146-013-0170-5.

Williams, T. G., and D. H. Turpin (1987), The role of external carbonic anhydrase in inorganic carbon acquisition by *Chlamydomonas reinhardii* at alkaline pH, *Plant Physiol.*, *83*(1), 92–96, doi:10.1104/pp.83.1.92.

Wu, Y., P. Li, B. Wang, C. Liu, M. He, and C. Chen (2008), Composition and activity of external carbonic anhydrase of microalgae from karst lakes in China, *Phycol. Res.*, *56*(2), 76–82, doi:10.1111/j.1440-1835.2008.00487.x.

Wu, Y. D., Y. Y. Wu, Q. Li and K. Zhao (2011), Effect of pH and fluoride on extracelluar carbonic anhydrase activity and photosynthetic efficiency of *Chlamydomonas Reinhardtii* and *Chlorella Pyrenoidosa*, *J. Agro-Environ. Sci. [in Chinese]*, *30*, 1972–1977.

Xiao, L., J. Hao, W. Wang, B. Lian, G. Shang, Y. Yang, C. Liu, and S. Wang (2014), The up-regulation of carbonic anhydrase genes of *Bacillus mucilaginosus* under soluble Ca^{2+} deficiency and the heterologously expressed enzyme promotes calcite dissolution, *Geomicrobiol. J.*, *31*, 632–641, doi:10.1080/01490451.2014.884195.

Xie, T., and Y. Wu (2014), The role of microalgae and their carbonic anhydrase on the biological dissolution of limestone, *Environ. Earth. Sci.*, *71*(12), 5231–5239, doi:10.1007/s12665-013-2925-7.

Yuan, D. X. (2001), On the karst ecosystem, *Acta Geol. Sin. (English ed.)*, *75*(3), 336–338, doi:10.1111/j.1755-6724.2001.tb00541.x.